

Fusion-Relevant Changes in Lipid Shape of Hydrated Cholesterol Hemisuccinate Induced by pH and Counterion Species

Benjamin Klasczyk,[†] Steffen Panzner,[‡] Reinhard Lipowsky,[†] and Volker Knecht*,[†]

Theory and Bio-Systems, Max Planck Institute of Colloids and Interfaces, 14424 Potsdam, Germany, and Novosom AG, Weinbergweg 22, 06120 Halle, Germany

Received: May 14, 2010; Revised Manuscript Received: September 1, 2010

Cholesterol hemisuccinate (CHEMS) is a protonable lipid that is frequently used for the construction of pH-responsive delivery systems. Such systems have a stable, lamellar phase at pH 7, but can form a fusogenic, hexagonal phase at pH 5. This behavior can be explained by binding or release of counterions from the solvent and the related variations of the effective size of the polar lipid part. Here, we use MD simulations to study the ion recruitment to neutral or anionic bilayers of CHEMS in water. For deprotonated (anionic) CHEMS, we observed an almost complete decoration of the bilayer with sodium, potassium, or argininium cations, which challenges the previous hypothesis that the stability of bilayers from anionic CHEMS results from the electrostatic repulsion between the charged head groups. Protonated (neutral) bilayers of CHEMS did not bind sodium or potassium, but did adsorb argininium cations. Whereas the headgroup of protonated CHEMS is bent and strongly tilted away from the bilayer normal, the headgroup of the deprotonated CHEMS is found to become outstretched and significantly less tilted arising from the adsorption of the counterions. The tilt reduction is most pronounced upon adsorption of arginine which also leads to an increase in the otherwise constant area per lipid. In general, the cation binding to the deprotonated CHEMS acts to increase the effective headgroup volume. This change in the lipid shape may be one possible fact explaining the hexagonal–lamellar phase transitions for CHEMS known from experiments.

Introduction

Delivery of bulky and highly polar molecules such as plasmids or oligonucleotides into cells requires the use of delivery systems, as these substances cannot penetrate cell membranes by themselves. A fundamental challenge is the transition between a stable complex of drug and delivery system outside the cell to its disassembly and directed release of cargo inside the cell.

One strategy to meet this challenge is to use pH-responsive liposomes that can adopt a lamellar, stable state at conditions of neutral pH outside of cells, but are able to undergo fusion upon acidification which occurs along the endosomal route. Cholesterol hemisuccinate (CHEMS) shown in Figure 1 is a lipid that undergoes such morphological transitions.¹ The pH-induced fusion is also observed in mixtures of CHEMS, and neutral lipids such as DOPE or cholesterol and such systems had attracted considerable interest as drug delivery systems.^{2–4} A significant drawback, however, is the limited ability of these deprotonated liposomes to encapsulate nucleic acids, which are negatively charged as well. This difficulty has been addressed in the recently introduced class of amphoteric liposomes,⁵ leading to a renewed interest in CHEMS and its pH-dependent polymorphism.

The polymorphic phase behavior of CHEMS is a function of its protonation state which changes around its pK. Hafez et al. reported a pK value of 5.8 in bilayers with 50 mol % POPC,¹ and we measured a pK of 5.4 in vesicles consisting of DMPC and CHEMS in a 70:30 ratio.⁶

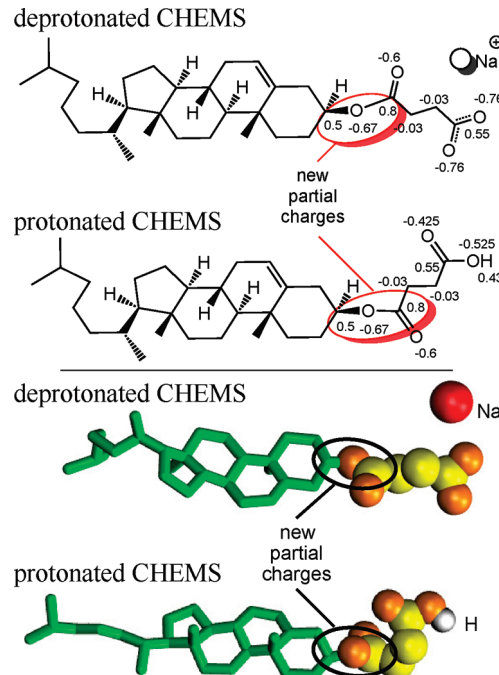


Figure 1. Chemical structure of protonated and deprotonated CHEMS in two different representations. Covalent bonds between carbons in the tail region are shown as green sticks and headgroup atoms or the sodium ion are shown as spheres. Here, oxygens are shown in orange, carbons in yellow, the carboxyl hydrogen in white, and sodium in red.

Mechanistically, the stabilization of the lamellar phase was explained by repulsion of the charged head groups, or by recruitment of counterions and the associated volume increment, or by a combination of both factors.^{1,6}

* To whom correspondence should be addressed: E-mail: vknecht@mpikg.mpg.de.

[†] Max Planck Institute of Colloids and Interfaces.

[‡] Novosom AG.

The fusion of CHEMS under conditions of low pH is well described. Additionally, we observed fusion of (charged) CHEMS bilayers at neutral or alkaline pH when the counterions were immobilized by means of ion exchange materials. Mass spectroscopy revealed significant binding of sodium at CHEMS liposomes at pH 7.5. These observations raise questions about the concept of an electrostatic stabilization of charged bilayers and indicate that membrane-bound ions play a dominant role in the stabilization of the lamellar phase. In this “ion switch” model, membrane-bound counterions contribute substantial volume to the polar lipid headgroup, thereby generating a lipid shape that generates a lamellar phase of the lipid assembly. Removal of counterions due to discharge of the lipid or the counterion itself causes a loss of headgroup volume and generates a lipid shape that promotes fusion.⁶

A powerful tool to study the interactions of ions with lipid bilayers in atomic detail is molecular dynamics (MD) simulations as demonstrated in numerous previous studies.^{7–12} For the first time, we have used MD simulations to study hydrated bilayers of CHEMS. We provide data that describe the ion attraction and concomitant headgroup enlargement of the charged lipid in the presence of sodium, potassium, or argininium cations. Surprisingly, the MD simulations describe a binding of argininium ions also to protonated bilayers of CHEMS, which might stabilize even uncharged CHEMS bilayers against fusion.

Methods

System Setup. All CHEMS bilayers in cation chloride solution were simulated using classical molecular dynamics techniques under periodic boundary conditions. Initial configurations of the CHEMS bilayers were constructed from the configuration of a single CHEMS molecule copied and translated in the *xy* direction to yield an 8×8 array of molecules. This monolayer was copied and rotated by 180° , yielding a bilayer configuration. This system was energy minimized using 50 000 steps of steepest descent first with flexible and subsequently with constrained bond lengths.

In the next step, the bilayer was hydrated such that the final bilayer was surrounded by 4926–7020 water molecules depending on the ion concentration. Sodium and potassium chlorides were added by randomly replacing water molecules varying from 0 to 200 ion pairs per system and for the deprotonated system with additional 128 counterions according to the number of lipids to neutralize the system. For systems containing arginine chlorides, arginines were first inserted randomly into the box containing only the CHEMS bilayer before the water was added. This procedure was followed by an energy minimization using 50 000 steps of steepest descent, first with flexible and subsequently with constrained bond lengths.

Water was described using the rigid simple point charge (SPC) model.^{13–15} The force field for the hydrophobic cholesterol fraction of CHEMS is taken from Holtje et al.¹⁶ This model is based on the widely used GROMOS87 force field¹⁷ in which hydrogens in hydrocarbon groups are treated implicitly using united atoms but with modified Lennard-Jones (LJ) interactions between the water oxygens and hydrocarbons. For the protonated carboxyl group of the succinate fraction, the hydrogen was considered explicitly. Partial charges for the succinate region were taken from ref 18 and parameters for bonded and LJ interactions from GROMOS87. Partial charges of the transition region between the cholesterol and succinate region were chosen as given in Table 1, using the ester bonds between the glycerol backbone and the fatty acid tails of Berger phospholipids¹⁹ as

TABLE 1: Partial Charges for Protonated and Deprotonated CHEMS

atoms	partial atomic charge	source
hydrophilic headgroup succinate fraction	see source	Dlugosz et al. ¹⁸
CH1	0.50	this work
OS	-0.67	
C	0.80	
hydrophobic tail cholesterol fraction	no charges	Holtje et al. ¹⁶

a template. Arginine was described using GROMOS87. For the alkali chlorides (Na^+ , K^+ , and Cl^-), parameters based on solution activities were used.^{20,21}

Each system was simulated for 100 ns at 300 K and 1 bar. The water molecules were kept rigid using SETTLE,²² and the lengths of covalent bonds in CHEMS or arginine were constrained using LINCS.²³ This facilitated the usage of a 2 fs time step for the integration of the equations of motion. The weak coupling technique by Berendsen et al. was used to control the temperature or pressure with relaxation times of 0.1 and 1.0 ps, respectively.²⁴ A pressure of 1 bar normal and lateral to the bilayer corresponding to a tension-free membrane were maintained by semi-isotropic scaling of the simulation box. Electrostatic interactions were evaluated using the particle mesh Ewald technique²⁵ with a 1 nm cutoff for direct space, a 0.12 nm grid spacing, and an interpolation order of 4. Neighbor lists were updated every five steps. All simulations were performed using the GROMACS package version 3.²⁶ Configurations were saved every 10 ps for analysis.

Analysis. The relaxation of the system was monitored from the time evolution of the potential energy. Depending on the cation chloride concentration the relaxation required 1–10 ns. This period was omitted in the further analysis. In the following, errors for numbers of next neighbors and contacts, areas per lipid, headgroup length, and the tilt angles give the standard error from block averages obtained by dividing the trajectory into five segments. The average number of water molecules or ions in contact with a given carboxyl or ester oxygen and the number of water molecules in contact with a given ion were determined considering the corresponding heavy atoms with a distance below a cutoff value. The latter was chosen as the position of the first minimum of the corresponding radial distribution function. The membrane thickness itself was determined from the distance between the maxima of the carboxyl group distributions of the two leaflets. The errors for the membrane thickness were evaluated from the width of the carboxyl group distributions. The head length was defined as the distance between the carboxyl group and the ester oxygens. The tilt of the lipid head was taken as the angle between the lipid head and the bilayer normal. The lipid volume was obtained from the product of the area per lipid and the membrane thickness. The effective head volume was determined from the area per lipid as well as the headgroup length and tilt assuming the head to correspond to a tilted cylinder. Electron densities for different parts of the system as a function of the position normal to the bilayer, z , were obtained by dividing the box in the z direction into 200 slices and smoothed by convoluting the profiles with a Gaussian distribution with a fwhm of about 1 nm.

Results

Molecular dynamics simulations of hydrated CHEMS bilayers in the protonated and deprotonated state for different ionic

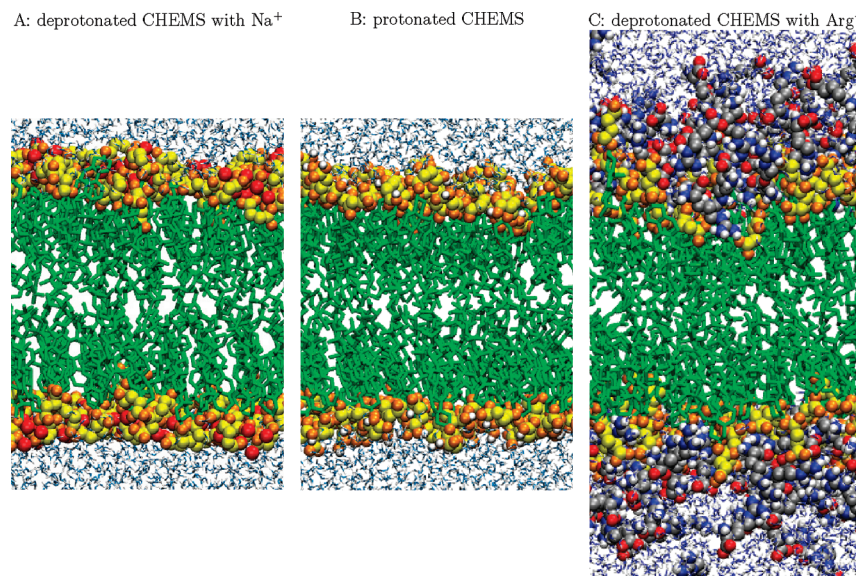


Figure 2. Cutout cross sections of hydrated CHEMS bilayers in (A) deprotonated state with sodium, (B) protonated state, or (C) deprotonated state with arginine, from molecular dynamics simulations. The representation of CHEMS and sodium is similar to that chosen in Figure 1. Water molecules are shown as sticks (blue water oxygen and white water hydrogen parts).

conditions have been conducted for the first time. The aim was to test assumptions underlying the dynamic lipid shape interpretation of pH-dependent fusion of CHEMS vesicles by Siepi et al.⁶ CHEMS bilayers were preconstructed and hydrated. Ions, if present, were distributed randomly in the water phase. From such configurations, a 100 ns simulation was started for each system. The final configurations for simulations of CHEMS in the protonated or deprotonated state with Na⁺ counterions are shown in Figure 2. For deprotonated CHEMS with only Na⁺ counterions (Figure 2A), almost all Na⁺ ions are adsorbed at CHEMS head groups. In effect, the size of the head groups is increased compared to the protonated state (Figure 2B).

The adsorption of Na⁺ at deprotonated CHEMS is also evident from the electron density profile in Figure 3A. The peaks in the sodium densities coincide with the peaks in the carboxyl carbon distribution. If excess NaCl is present, additional Na⁺ is adsorbed, leading to the formation of a layer of Cl⁻ counterions at the water side as shown in Figure 3B. Apparently, adsorption does not arise from a compensation of lipid charge alone but overcompensates the lipid charge, a process known as charge inversion.²⁷ Arg⁺ as a counterion gets also strongly adsorbed at the head groups (Figure 3C). Compared to Na⁺, it is very bulky, as reflected by the corresponding broader and higher peak at the interface leading to a strong depletion of water. For excess ArgCl, the arginine distribution decays very slowly toward the water phase. Arg⁺ also overcompensates the lipid charge, leading to the formation of a more diffuse layer of Cl⁻ counterions.

For protonated CHEMS, excess NaCl remains uniformly distributed in the water phase (Figure 3F). In contrast to Na⁺, excess ArgCl is adsorbed at the protonated CHEMS bilayer (Figure 3G). The adsorption of arginine at the interface may be facilitated due to the amphiphilic nature of arginine, comprising the charged NH₃⁺ and COO⁻ termini of its backbone and the cationic guanidinium group of the side chain on the one hand and a three-carbon aliphatic chain on the other hand. It is known that arginine adsorbs at zwitterionic phospholipid bilayers.^{28–30}

The adsorption of ions in terms of contacts to lipid head groups is indicated in Table 2. The table gives the number of water molecules in the first hydration shell of carboxyl and ester

oxygens and the cations, as well as the number of ions in contact with a given carboxyl or ester oxygen. For protonated CHEMS, a given carboxyl oxygen is in contact with a cation for a fraction of 0.001–0.7 of the length of the trajectory depending on the cation. Carboxyl oxygens are more often in contact with arginine as with sodium or potassium. The number of cations at the carboxyl groups increases with increasing ion concentration.

For deprotonated CHEMS, carboxyl groups are in contact with about two sodium or potassium ions. Figure 4 shows that this is due to the formation of CHEMS–cation complexes with 2:2 stoichiometry. In contrast, carboxyl groups contact only one arginine molecule, here, apparently, the formation of 2:2 complexes is sterically hindered.

The hydration numbers of 5.2–5.6 and 6.6–7.0 for sodium and potassium, respectively, in the *protonated* CHEMS system are comparable to the corresponding hydration numbers for ions in bulk solution from previous simulations with the same ion force field as given by 4.9–5.5 for Na⁺ and 7–8 for K⁺,^{20,21} which indicates that the cations interact only weakly with protonated CHEMS. For *deprotonated* CHEMS, the hydration numbers of these cations are decreased by around 2.8–4.1 for sodium and 2.7–4.7 for potassium. Hence, upon adsorption at the charged carboxyl groups of the lipids the ions become partially dehydrated. Partial dehydration has also been observed for adsorption of ions at phospholipid bilayers in previous simulations.^{11,31}

The carboxyl oxygens are always somewhat more strongly hydrated than the ester oxygens, as expected from the fact that the latter reside more deeply in the bilayer. For protonated CHEMS at increasing ion concentration, the hydration of the ester oxygen is constant or slightly increases. With increasing cation size the hydration of the carboxyl group decreases, presumably due to steric effects. For deprotonated CHEMS, the hydration of the carboxyl group decreases between 0 and 0.5 mol/L and increases between 0.5 and 1 mol/L with increasing concentration of sodium or potassium. The change in trend at high compared to low ion concentrations might arise from ion–ion correlations (present at high but not at low ion concentrations). The decrease in hydration numbers correlates with the increase in contacts of carboxyl oxygens with ions, indicating the partial replacement of water by ions. In the

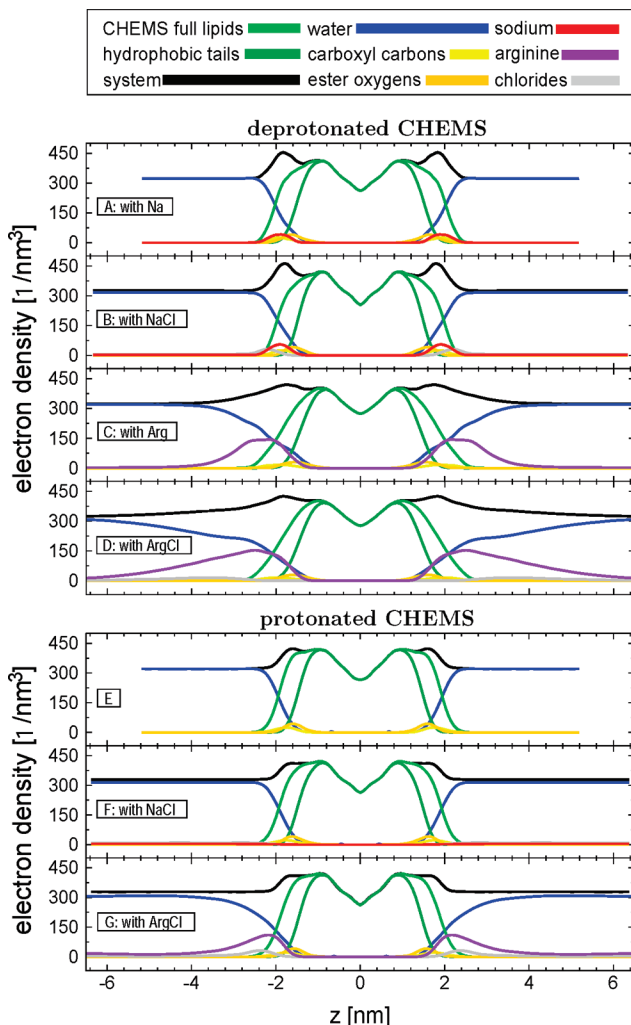


Figure 3. (Partial) electron density profiles for (A–D) deprotonated CHEMS with counterions or (E–G) protonated CHEMS, either without or with 100 sodium or arginine chlorides. The cation profiles show accumulation at the water lipid interface depending on the concentration.

presence of arginine, the carboxyl oxygens are less strongly hydrated than in the presence of the atomic cations.

Figure 5 compares the effect of protonation state and ions on the geometry of the bilayer in terms of the membrane thickness, the area per lipid, the head length, and the tilt angle. The observed membrane thickness depends neither on the type nor on the concentration of the ions but may depend on the protonation state: deprotonated CHEMS bilayers are systematically thicker by 0.5 nm, even though this difference is within the estimated errors.

The area per lipid in the protonated state is in the range $0.365\text{--}0.375 \text{ nm}^2$. For deprotonated CHEMS in the presence of NaCl or KCl, the area per lipid is similar. An increase in the area per lipid to values in the range $0.38\text{--}0.39 \text{ nm}^2$ is seen in the presence of ArgCl. The molecular areas per lipid for CHEMS are comparable to the area per lipid of $0.39 \pm 0.01 \text{ nm}^2$ in compressed (30 mN/m) cholesterol monolayers at the water/air interface.³² These values indicate that the packing density of CHEMS is mainly determined by the hydrophobic segment, which is the same as for cholesterol.

The headgroup length is in the range $0.395\text{--}0.41 \text{ nm}$ for protonated CHEMS and increased for deprotonated CHEMS to values in the range $0.415\text{--}0.425 \text{ nm}$ in the presence of NaCl

TABLE 2: Number of Water Oxygens (Ow) in the First Hydration Shell of Carboxyl (Oc) and Ester Oxygens and the Cations (Ion), as Well as the Number of Ions in Contact with a Given Carboxyl or Ester Oxygen^a

deprotonated CHEMS						
ions	in mol/L	Oc–Ow	Oe–Ow	ion–Ow	Oc–ion	Oe–ion
only Na	0.000	0.583	0.400	0.988	2.072	0.115
only K	0.000	0.730	0.338	0.801	1.909	0.121
only Arg	0.000	2.725	0.227	5.561	0.614	0.133
NaCl	0.028	0.521	0.382	1.104	2.176	0.131
	0.112	0.441	0.384	1.424	2.238	0.145
	0.198	0.396	0.361	1.642	2.347	0.138
	0.507	0.367	0.349	2.261	2.383	0.159
	1.096	1.862	0.332	2.842	2.417	0.144
KCl	0.021	0.696	0.288	2.263	2.348	0.268
	0.054	0.487	0.258	2.525	2.475	0.232
	0.145	0.472	0.258	2.793	2.530	0.233
	0.382	0.351	0.254	3.518	2.591	0.195
	1.046	1.813	0.252	4.312	2.563	0.205
ArgCl	0.010	2.680	0.228	12.203	1.135	0.268
	0.047	2.684	0.234	11.772	1.140	0.305
	0.603	2.684	0.237	11.714	1.131	0.305
	1.337	2.631	0.244	12.294	1.131	0.263
	5.812	2.579	0.206	11.779	1.152	0.267
protonated CHEMS						
ions	in mol/L	Oc–Ow	Oe–Ow	ion–Ow	Oc–ion	Oe–ion
no ions	0.000	0.685	0.275	0.000	0.000	0.000
NaCl	0.080	0.698	0.235	5.562	0.001	0.009
	0.241	0.684	0.244	5.566	0.002	0.015
	0.403	0.666	0.245	5.528	0.004	0.023
	0.814	0.691	0.244	5.417	0.008	0.051
	1.644	0.700	0.241	5.208	0.017	0.091
KCl	0.066	0.558	0.237	6.638	0.023	0.004
	0.203	0.538	0.224	6.703	0.067	0.014
	0.353	0.559	0.230	6.815	0.101	0.011
	0.722	0.556	0.228	6.962	0.137	0.026
	1.445	0.521	0.180	6.880	0.202	0.031
ArgCl	0.091	0.377	0.384	12.491	0.129	0.016
	0.071	0.308	0.245	10.603	0.282	0.025
	0.166	0.268	0.243	11.481	0.455	0.061
	1.827	0.262	0.207	12.192	0.515	0.075
	3.819	0.229	0.210	12.341	0.674	0.084

^a Relative errors lie within the range 1–6%.

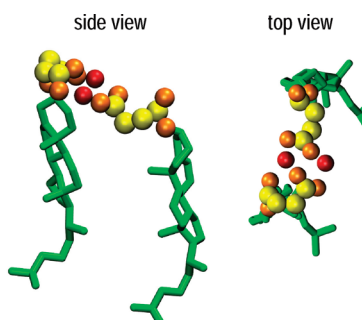


Figure 4. MD simulation snapshot of two different orientations of a CHEMS–sodium complex with a 2:2 stoichiometry for the deprotonated state of the lipid. The color code is explained in Figure 1. The formation of such complexes is also indicated from the coordination number of approximately two for CHEMS carboxyl oxygens with sodium given in Table 2.

or KCl and 0.435 nm in the presence of ArgCl. The headgroup of protonated CHEMS is tilted from the bilayer normal by $55\text{--}58^\circ$. The tilt is smaller for deprotonated CHEMS, and depends on the counterion species, decreasing in the order Na^+ , K^+ , Arg⁺.

As shown in Figure 6, the lipid headgroup volume depends on the protonation state and the counterion species. For protonated CHEMS, the headgroup volume is around 0.08 nm^3 in the presence of Na^+ or K^+ while somewhat increased to 0.085

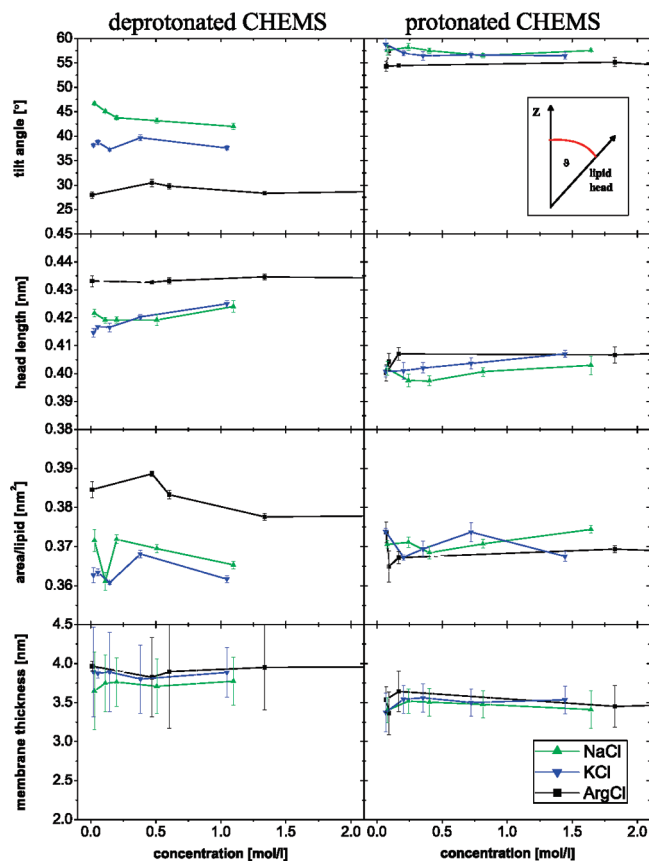


Figure 5. Membrane thickness, area per lipid, lipid head length, and the tilt angles for deprotonated and protonated CHEMS in the presence of sodium, potassium, or arginine chloride as a function of ion concentration. The tilt angle of the headgroup is substantially reduced for the deprotonated CHEMS lipids. The size of the reduction depends on the size of the bare cation.

nm³ in the presence of Arg⁺. For deprotonated CHEMS, the headgroup volume is overall increased to values around 0.11, 0.12, or 0.145 nm³ in the presence of Na⁺, K⁺, or Arg⁺, respectively. In contrast, the lipid tail volume is essentially the same for all conditions.

The increase in headgroup length upon deprotonation and adsorption of arginine reflects a transition from a bent to an outstretched conformation of the headgroup. This and the concomitant decrease in the headgroup tilt are reflected in the configurations shown in Figure 1.

Conclusion

Our MD simulations show that deprotonation of CHEMS leads to strong adsorption of counterions (Na⁺, K⁺, or Arg⁺) at the carboxyl groups. Ion binding is accompanied by a stretching and more vertical orientation of the headgroup. Sterically, the associated ion becomes part of the headgroup volume, which leads to a substantial increase of this parameter. Following shape arguments, this increased headgroup size should promote a lamellar phase and suppress fusion. Whereas the classical theory does not consider bound ions, their recruitment or release provides a consistent explanation for the phase transition observed upon protonation of CHEMS. The data obtained here demonstrate that the ion occupancy of charged CHEMS is almost complete—a fact that adds importance on molecular shape, but de-emphasizes electrostatic contributions. Indeed, for a pH at which CHEMS is deprotonated and exhibits a large headgroup as shown here, CHEMS does form vesicles that are

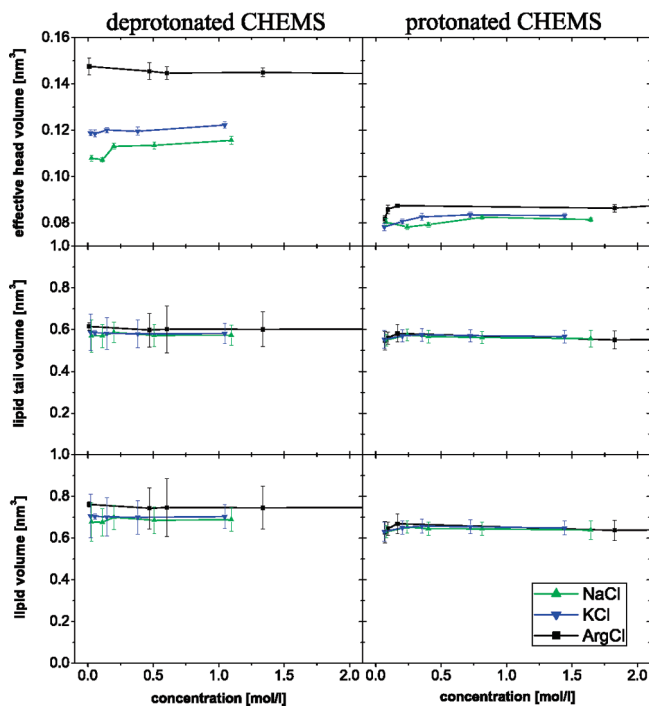


Figure 6. Volumes of lipid, lipid tail, and lipid head for deprotonated and protonated CHEMS in the presence of sodium, potassium, or arginine chloride, as a function of ion concentration. The head volume is significantly larger for deprotonated than for protonated CHEMS lipids and depends on the size of the positively charged counterion.

stable against fusion in experiment.⁶ Also, Arg⁺, shown here to lead to a headgroup size larger than in the presence of Na⁺ or K⁺, is found to suppress fusion more efficiently than the other two ion species.⁶ Our simulations thus support the dynamic shape interpretation introduced by Siepi et al.⁶

Adsorbed ions are found to be partially dehydrated. This is similar to what has been observed for adsorption of ions on phospholipid bilayers.^{11,31} Notably, we find that adsorption of Arg⁺ leads to a pronounced increase in the area per lipid. This prediction could be tested experimentally for monolayers at a water/air interface.

Furthermore, protonated CHEMS does not adsorb Na⁺ or K⁺ ions, as assumed in the dynamic shape interpretation. Similar to phospholipids,^{28–30} protonated CHEMS does adsorb arginine. This leads to an increase in headgroup volume which, in turn, is expected to suppress fusion. This prediction could also be tested experimentally, as a further validation of the dynamic lipid shape interpretation.

References and Notes

- (1) Hafez, I. M.; Cullis, P. R. *Biochim. Biophys. Acta, Biomembr.* **2000**, 1463, 107–114.
- (2) Ellens, H.; Bentz, J.; Szoka, F. C. *Biochemistry* **1984**, 23, 1532–1538.
- (3) Slepushkin, V. A.; Simoes, S.; Dazin, P.; Newman, M. S.; Guo, L. S.; de Lima, M. C. P.; Düzgünes, N. *J. Biol. Chem.* **1997**, 272, 2382.
- (4) Zhang, J. X.; Zalipsky, S.; Mullah, N.; Pechar, M.; Allen, T. M. *Pharmacol. Res.* **2004**, 49, 185–198.
- (5) Andreakos, E.; Rauchhaus, U.; Stavropoulos, A.; Endert, G.; Wendisch, V.; Benahmed, A. S.; Giaglis, S.; Karras, J.; Lee, S.; Gaus, H.; Bennett, C. F.; Williams, R. O.; Sideras, P.; Panzner, S. *Arthr. Care Res.* **2009**, 60, 994–1005.
- (6) Siepi, E.; Lutz, S.; Reinsch, C.; Panzner, S. An ion switch regulates membrane fusion and allows the rational design of cellular transfectants; submitted for publication, 2010.
- (7) Pandit, S. A.; Bostick, D.; Berkowitz, M. L. *Biophys. J.* **2003**, 84, 3743–3750.

- (8) Sachs, J. N.; Nanda, H.; Petracche, H. I.; Woolf, T. B. *Biophys. J.* **2004**, *86*, 3772–3782.
- (9) Gurtovenko, A. A. *J. Chem. Phys.* **2005**, *122*, 244902.
- (10) Gurtovenko, A. A.; Vattulainen, I. *J. Phys. Chem. B* **2008**, *112*, 1953.
- (11) Böckmann, R. A.; Hac, A.; Heimburg, T.; Grubmüller, H. *Biophys. J.* **2003**, *85*, 1647–1655.
- (12) Vacha, R.; Siu, S. W. I.; Petrov, M.; Böckmann, R. A.; Barucha-Kraszewska, J.; Jurkiewicz, P.; Hof, M.; Berkowitz, M. L.; Jungwirth, P. *J. Phys. Chem. A* **2009**, *113*, 7235–7243.
- (13) Berendsen, H. J. C.; Postma, J. P. M.; van Gunsteren, W. F.; Hermans, J. Interaction models for water in relation to protein hydration. In *Intermolecular Forces*; Pullman, B., Ed.; D. Reidel Publishing Co.: Dordrecht, The Netherlands, 1981; pp 331–342.
- (14) Jorgensen, W. L.; Chandrasekhar, J.; Madura, J. D.; Impey, R. W.; Klein, M. L. *J. Chem. Phys.* **1983**, *79*, 926–935.
- (15) Hermans, J.; Berendsen, H. J. C.; van Gunsteren, W. F.; Postma, J. P. M. *Biopolymers* **1984**, *23*, 1513–1518.
- (16) Höltje, M.; Förster, T.; Brandt, B.; Engels, T.; von Rybinski, W.; Höltje, H. D. *Biochim. Biophys. Acta, Biomembr.* **2001**, *1511*, 156–167.
- (17) van Gunsteren, W. F.; Berendsen, H. J. C. *Groningen molecular simulation (GROMOS) library manual*; Biomos b.v.: Groningen, The Netherlands, 1987.
- (18) Drugosz, M.; Antosiewicz, J. M. *J. Chem. Phys.* **2004**, *302*, 161–170.
- (19) Berger, O.; Edholm, O.; Jähnig, F. *Biophys. J.* **1997**, *72*, 2002–2013.
- (20) Weerasinghe, S.; Smith, P. E. *J. Chem. Phys.* **2003**, *119*, 11342.
- (21) Klasczyk, B.; Knecht, V. *J. Chem. Phys.* **2010**, *132*, 24109.
- (22) Miyamoto, S.; Kollman, P. A. *J. Comput. Chem.* **1992**, *13*, 952–962.
- (23) Hess, B.; Bekker, H.; Berendsen, H. J. C.; Fraaije, J. G. E. M. *J. Comput. Chem.* **1997**, *18*, 1463–1472.
- (24) Berendsen, H. J. C.; Postma, J. P. M.; van Gunsteren, W. F.; DiNola, A.; Haak, J. R. *J. Chem. Phys.* **1984**, *81*, 3684.
- (25) Darden, T.; York, D.; Pedersen, L. *J. Chem. Phys.* **1993**, *98*, 10089.
- (26) van der Spoel, D.; Lindahl, E.; Hess, B.; Groenhof, G.; Mark, A. E.; Berendsen, H. J. C. *J. Comput. Chem.* **2005**, *26*, 1701–1718.
- (27) Lyklema, J. *Colloids Surf., A: Physicochem. Eng. Asp.* **2006**, *291*, 3–12.
- (28) MacCallum, J. L.; Bennett, W. F. D.; Tielemans, D. P. *Biophys. J.* **2008**, *94*, 3393–3404.
- (29) Yoshida, Y.; Maeda, K.; Shirai, O. *J. Electroanal. Chem.* **2005**, *578*, 17–24.
- (30) Tang, M.; Waring, A. J.; Hong, M. *J. Am. Chem. Soc.* **2007**, *129*, 11438–11446.
- (31) Cordomi, A.; Edholm, O.; Perez, J. J. *J. Phys. Chem. B* **2008**, *112*, 1397–1408.
- (32) Baglioni, P.; Cestelli, G.; Dei, L.; Gabrielli, G. *J. Colloid Interface Sci.* **1985**, *104*, 143–150.

JP1043943